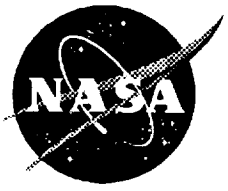


1N-34
13716
36p

NASA Contractor Report 194918

ICASE Report No. 94-36



ICASE

A FAST NUMERICAL SOLUTION OF SCATTERING BY A CYLINDER: SPECTRAL METHOD FOR THE BOUNDARY INTEGRAL EQUATIONS

Fang Q. Hu

(NASA-CR-194918) A FAST NUMERICAL SOLUTION OF SCATTERING BY A CYLINDER: SPECTRAL METHOD FOR THE BOUNDARY INTEGRAL EQUATIONS Final Report (ICASE) 36 p

N94-34949

Unclass

G3
34 0013716

Contract NAS1-19480
May 1994

Institute for Computer Applications in Science and Engineering
NASA Langley Research Center
Hampton, VA 23681-0001



Operated by Universities Space Research Association

A fast numerical solution of scattering by a cylinder : Spectral Method for the Boundary Integral Equations

FANG Q. HU

Department of Mathematics and Statistics, Old Dominion University

Norfolk, VA 23529

Abstract

It is known that the exact analytic solutions of wave scattering by a circular cylinder, when they exist, are not in a closed form but in infinite series which converges slowly for high frequency waves. In this paper, we present a fast numerical solution for the scattering problem in which the Boundary Integral Equations, reformulated from the Helmholtz equation, are solved using a Fourier spectral method. It is shown that the special geometry considered here allows the implementation of the spectral method to be simple and very efficient. The present method differs from previous approaches in that the singularities of the integral kernels are removed and dealt with accurately. The proposed method preserves the spectral accuracy and is shown to have an exponential rate of convergence. Aspects of efficient implementation using FFT are discussed. Moreover, the boundary integral equations of combined single and double-layer representation are used in the present paper. This ensures the uniqueness of the numerical solution for the scattering problem at all frequencies. Although a strongly singular kernel is encountered for the Neumann boundary conditions, we show that the hypersingularity can be handled easily in the spectral method. Numerical examples that demonstrate the validity of the method are also presented.

This work was supported by the National Aeronautics and Space Administration under NASA Contract NAS1-19480 while the author was in residence at the Institute for Computer Applications in Science and Engineering, NASA Langley Research Center, Hampton, VA 23665, USA.



INTRODUCTION

The exact analytic solutions of wave scattering by a circular cylinder, obtainable for simple incident waves, are not in a closed form but in infinite series of Bessel and Hankel functions of increasing orders. Such solutions converge slowly, especially for high frequency waves, which render their numerical evaluation inefficient. This paper presents a fast numerical solution of wave scattering that only requires the computation of Bessel and Hankel functions of order zero. Furthermore, the numerical solution is valid for any form of the incident waves of all frequencies.

When developing numerical solutions, wave scattering problems are often conveniently formulated in Boundary Integral Equations (BIE)¹. The advantages of the Boundary Integral Equation Method (BIEM) include reducing the dimension of the problem and transforming an infinite domain to finite boundaries in which the far field radiation condition is satisfied automatically. The Boundary Integral Equations are commonly solved computationally by the Boundary Element Methods (BEM)². In this method the boundary is divided into finite elements and integrations over each boundary element are approximated by quadratures, e.g. the linear elements.

In this paper, we develop a Spectral Method of solving the Boundary Integral Equations, reformulated from the Helmholtz equation, for numerical solutions of wave scattering by a circular cylinder. Previously, for this special geometry, a “fast numerical method” based on the Fourier approximations has been formulated by Bojarski³, who pointed out that the boundary integral equation of wave scattering can be solved easily and efficiently in the Fourier spectrum domain of the solution. Due to the simplicity of the geometry, an *explicit* relation between the Fourier coefficients of the solution and those of the boundary condition was found. It was argued that the numerical

approach was more efficient than directly evaluating the infinite series of the exact solutions. Indeed, the exact solutions contain Bessel and Hankel functions of higher orders whose numerical evaluation is more difficult and costly as the order increases. Recently a similar approach has been used and extended by Schuster⁴ for a wave transmission problem of concentric cylinders.

In the present paper, we point out that the numerical formulations given previously are not achieving the optimal accuracy of the Fourier spectral methods. It is known that, although any periodic function can be approximated by a truncated Fourier series, the rate of convergence of such an approximation depends on its smoothness. Unfortunately, the integral kernels for the Helmholtz equation are not smooth. In particular, the 2-D Green's function of the Helmholtz equation, appearing in the integral equations, possesses a logarithmic singularity. Furthermore, the normal derivative of the Green's function also contains a term involving the logarithmic function. The non-smoothness of the integral kernels, however, was not explicitly treated in the previous formulations. It will be seen that it is critical to remove the non-smoothness of the integral kernels in order to achieve fast convergence in the Fourier spectral formulation. By a proper treatment of the singularities, the present numerical formulation yields accurate solutions with significantly fewer datum points. Moreover, the boundary integral equations of combined single and double-layer representation are used in the present paper. This ensures the uniqueness of the numerical solution for the scattering problem at all frequencies^{1,5}. Although a combined layer formulation results in a strongly singular kernel for the Neumann boundary conditions, we show that the hypersingularity is handled easily in the spectral method.

In the next section, the formulations of the Boundary Integral Equations for wave

scattering problems are given. Then, in sections II and III, the Fourier spectral methods for the Dirichlet and Neumann boundary conditions are presented. Numerical results are shown in section IV. Section V contains the conclusions. Some analytic results are also given in the Appendix.

I. BOUNDARY INTEGRAL EQUATIONS

Let us consider wave scattering by a circular cylinder Γ of radius a . The wave equation for the scattered function ϕ with assumed time dependency of $e^{-i\omega t}$ is reduced to the Helmholtz equation

$$\nabla^2 \phi + \kappa^2 \phi = 0 \quad (1)$$

where $\kappa = \omega/c$ (c is the wave speed) and ∇^2 is the 2-D Laplace operator $\nabla^2 = \frac{\partial^2}{\partial x^2} + \frac{\partial^2}{\partial y^2}$. The boundary condition considered in this paper will be one of the following types :

$$\textit{Dirichlet(soft)} : \quad \phi(\vec{r}) = b(\vec{r}) \quad \text{On } \Gamma$$

or

$$\textit{Neumann(hard)} : \quad \frac{\partial \phi}{\partial \mathbf{n}}(\vec{r}) = b(\vec{r}) \quad \text{On } \Gamma$$

The Helmholtz equation (1) together with the boundary condition can be reformulated into a Boundary Integral Equation. This can be done in various ways^{1,5}. For scattering problems considered in the present paper, we use a combination of single and double-layer formulation in which the solution ϕ at any point \vec{r}' in the scattered field is represented by an integral on the boundary as⁵

$$\phi(\vec{r}') = \int_{\Gamma} \left(\frac{\partial G}{\partial \mathbf{n}} - i\eta G \right) f(\vec{r}) d\Gamma \quad (2)$$

where η is any real number such that

$$\eta \operatorname{Re}(\kappa) > 0$$

The use of a combined formulation ensures the uniqueness of the numerical solution for exterior problems^{1,5}. In (2), $f(\vec{r})$ is an unknown layer distribution function and the Green's function $G(\vec{r}, \vec{r}')$, whose form will be given later, satisfies the following equation

$$\nabla^2 G + \kappa^2 G = -\delta(\vec{r} - \vec{r}') \quad (3)$$

Here the normal derivative $\frac{\partial}{\partial \mathbf{n}}$ is assumed to be taken in the direction outward from the cylinder.

The Boundary Integral Equation associated with the layer representation (2) is⁵

$$\frac{1}{2}f(\vec{r}'_{\Gamma}) + \int_{\Gamma} \left(\frac{\partial G}{\partial \mathbf{n}} - i\eta G \right) f(\vec{r}_{\Gamma}) d\Gamma = b(\vec{r}'_{\Gamma}) \quad (4a)$$

for *Dirichlet boundary conditions* and

$$\frac{i\eta}{2}f(\vec{r}'_{\Gamma}) + \int_{\Gamma} \left(\frac{\partial^2 G}{\partial \mathbf{n}' \partial \mathbf{n}} - i\eta \frac{\partial G}{\partial \mathbf{n}'} \right) f(\vec{r}_{\Gamma}) d\Gamma = b(\vec{r}'_{\Gamma}) \quad (4b)$$

for *Neumann boundary conditions*, respectively. In (4a) and (4b), \vec{r}_{Γ} denotes the boundary points. After the layer distribution function f has been solved from the integral equation (4a) or (4b), the solution of the Helmholtz equation ϕ is found by the boundary integral (2).

Now for a circular cylinder of radius a , the boundary contour can be expressed as

$$\vec{r}_{\Gamma}(\theta) = (a \cos \theta, a \sin \theta), \quad 0 \leq \theta \leq 2\pi \quad (5)$$

The normal vector to be used in (4a) and (4b) is $\mathbf{n} = (\cos \theta, \sin \theta)$.

The Green's function and its normal derivative are^{5,6}

$$G = \frac{i}{4} H_0^{(1)} \left(\kappa |\vec{r}_\Gamma(\theta) - \vec{r}_\Gamma(\theta')| \right) = \frac{i}{4} H_0^{(1)} \left(2\kappa a \left| \sin \frac{\theta - \theta'}{2} \right| \right) \quad (6)$$

and

$$\begin{aligned} \frac{\partial G}{\partial \mathbf{n}} &= -\frac{i\kappa}{4} H_1^{(1)} \left(\kappa |\vec{r}_\Gamma(\theta) - \vec{r}_\Gamma(\theta')| \right) \frac{(\vec{r}_\Gamma(\theta) - \vec{r}_\Gamma(\theta')) \cdot \mathbf{n}}{|\vec{r}_\Gamma(\theta) - \vec{r}_\Gamma(\theta')|} \\ &= -\frac{i\kappa}{4} H_1^{(1)} \left(2\kappa a \left| \sin \frac{\theta - \theta'}{2} \right| \right) \left| \sin \frac{\theta - \theta'}{2} \right| \end{aligned} \quad (7)$$

in which we have used the fact that $|\vec{r}_\Gamma(\theta) - \vec{r}_\Gamma(\theta')| = 2a \left| \sin \frac{\theta - \theta'}{2} \right|$.

It is important to note here that G and $\frac{\partial G}{\partial \mathbf{n}}$ are functions of $\theta - \theta'$. As will be seen later, this allows the implementation of the Fourier spectral method to take a simple form.

We thus express the boundary integral equation (4a) for the Dirichlet boundary conditions as

$$\frac{1}{2} f(\theta') + \int_0^{2\pi} \left(\frac{\partial G}{\partial \mathbf{n}}(\theta - \theta') - i\eta G(\theta - \theta') \right) f(\theta) a d\theta = b(\theta') \quad (8a)$$

and equation (4b) for the Neumann boundary conditions as

$$\frac{i\eta}{2} f(\theta') + \int_0^{2\pi} \left(\frac{\partial^2 G}{\partial \mathbf{n}' \partial \mathbf{n}}(\theta - \theta') - i\eta \frac{\partial G}{\partial \mathbf{n}'}(\theta - \theta') \right) f(\theta) a d\theta = b(\theta') \quad (8b)$$

For clarity, the dependencies on θ and θ' have been expressed explicitly in (8a) and (8b).

In the next two sections, we give the numerical formulations of solving the integral equations (8a) and (8b) by a Fourier spectral method. Since different types of singularities are encountered, the two equations will be dealt with separately.

II. SPECTRAL METHOD FOR DIRICHLET BOUNDARY CONDITIONS

A. Formulation

Let the layer distribution function $f(\theta)$ and the boundary condition $b(\theta)$ be approximated by the truncated Fourier series as

$$f(\theta) = \sum_{n=-N/2}^{N/2-1} f_n e^{in\theta} \quad (9)$$

$$b(\theta) = \sum_{n=-N/2}^{N/2-1} b_n e^{in\theta} \quad (10)$$

where b_n are obtained by the FFT from prescribed boundary condition and f_n are the unknown coefficients. In (9) and (10), the particular form of truncated Fourier series has been taken for the convenience of applying FFT programs.

Substituting (9) and (10) into the boundary integral equation for the Dirichlet boundary conditions (8a), we get

$$\frac{1}{2} \sum_{n=-N/2}^{N/2-1} f_n e^{in\theta'} + \sum_{n=-N/2}^{N/2-1} \left[f_n \int_0^{2\pi} \left(\frac{\partial G}{\partial \mathbf{n}}(\theta - \theta') - i\eta G(\theta - \theta') \right) e^{in\theta} a d\theta \right] = \sum_{n=-N/2}^{N/2-1} b_n e^{in\theta'} \quad (11)$$

For simplicity, let

$$x = \theta - \theta'$$

By equating the coefficients of $e^{in\theta'}$, equation (11) is easily reduced to

$$\frac{1}{2} f_n + f_n \int_0^{2\pi} \left(\frac{\partial G}{\partial \mathbf{n}}(x) - i\eta G(x) \right) e^{inx} a dx = b_n \quad (12)$$

for $-N/2 \leq n \leq N/2 - 1$.

It is seen that the integral appearing in (12) are related to the Fourier coefficients of $\frac{\partial G}{\partial \mathbf{n}}(x)$ and $G(x)$. From (6) and (7), it is also clear that both are *periodic* functions of

x , with a period of 2π . Thus if we let $G(x)$ and $\frac{\partial G}{\partial \mathbf{n}}(x)$ be approximated by truncated Fourier series as

$$G(x) = \sum_{n=-N/2}^{N/2-1} g_n e^{-inx} \quad (13)$$

$$\frac{\partial G}{\partial \mathbf{n}}(x) = \sum_{n=-N/2}^{N/2-1} h_n e^{-inx} \quad (14)$$

then, the integral in (12) equals to $2\pi a(h_n - i\eta g_n)$. It follows that

$$\frac{1}{2}f_n + 2\pi a f_n (h_n - i\eta g_n) = b_n \quad (15)$$

Therefore, the Fourier coefficients of the layer distribution function $f(\theta)$ are obtained *explicitly* as

$$f_n = \frac{b_n}{\frac{1}{2} + 2\pi a (h_n - i\eta g_n)} \quad (16)$$

The above equation shows that once the Fourier coefficients of $G(x)$ and $\frac{\partial G}{\partial \mathbf{n}}(x)$ have been found, the layer distribution function $f(\theta)$ is known immediately.

Actually, the Fourier coefficients of $G(x)$ and $\frac{\partial G}{\partial \mathbf{n}}(x)$ can be found in exact form using higher order Bessel and Hankel functions. They are derived in Appendix A. Nonetheless, the numerical evaluation of the exact expressions becomes more ineffective and costly as the order of the special functions increases. In what follows we give the numerical method that computes the Fourier coefficients g_n and h_n accurately and efficiently.

B. Computation of g_n and h_n

In general, the Fourier coefficients of a periodic function can be obtained efficiently by using a Fast Fourier Transform algorithm (FFT). However, the accuracy of the

Fourier coefficients computed by the FFT using a given number of datum points depends on the smoothness of the function. Only when the function is infinitely smooth (i.e. infinitely differentiable), the error of Fourier coefficients computed by FFT decays faster than any power of $1/N$, where N is the number of datum points. Such a convergence is often referred to as an *exponential convergence* and the method is said to have *spectral accuracy*^{7,8}. Our aim here is to compute g_n and h_n by the FFT with *spectral accuracy* even though the functions G and $\frac{\partial G}{\partial \mathbf{n}}$ are not smooth.

In the numerical approaches proposed previously^{3,4}, the Fourier coefficients g_n and h_n were computed directly as the FFT of the $G(x)$ and $\frac{\partial G}{\partial \mathbf{n}}(x)$ respectively. However, the Green's function $G(x)$ has a logarithmic singularity at $x = 0$, where $\theta = \theta'$, due to the Hankel function of order zero in (6), and its Fourier series converges at the rate of $1/N$. Thus direct computation of g_n from $G(x)$ using FFT yields results whose accuracy is only comparable to a first order method. Furthermore, the function $\frac{\partial G}{\partial \mathbf{n}}(x)$ also has a non-smooth derivative at $x = 0$, and its Fourier series converges at the rate of $1/N^3$. Thus direct computation of h_n from $\frac{\partial G}{\partial \mathbf{n}}(x)$ is only comparable to a third order method. Alternatively, as will be shown below, by properly treating the non-smoothness of $G(x)$ and $\frac{\partial G}{\partial \mathbf{n}}(x)$, g_n and h_n are computed with spectral accuracy.

To examine the singularity of $G(x)$, we note that

$$G(x) = \frac{i}{4} H_0^{(1)} \left(2\kappa a \left| \sin \frac{x}{2} \right| \right) = \frac{i}{4} \left[J_0 \left(2\kappa a \left| \sin \frac{x}{2} \right| \right) + i Y_0 \left(2\kappa a \left| \sin \frac{x}{2} \right| \right) \right]$$

in which J_0 and Y_0 are the zeroth order Bessel functions of the first and second kind, respectively. Using the asymptotic series for small arguments, we have⁹

$$J_0(z) = 1 - \frac{z^2}{4} + \frac{z^4}{64} - \dots$$

$$Y_0(z) = \frac{2}{\pi} \ln \left(\frac{z}{2} \right) J_0(z) + \frac{2\gamma}{\pi} J_0(z) + \frac{z^2}{2\pi} - \dots$$

It follows that, for $|x|$ small,

$$G(x) = -\frac{1}{2\pi} \ln \left(\kappa a \left| \sin \frac{x}{2} \right| \right) J_0 \left(2\kappa a \left| \sin \frac{x}{2} \right| \right) - \frac{\gamma}{2\pi} + \frac{i}{4} + O(x^2) \quad (17)$$

in which $O(x^2)$ represents a power series in x^2 , and γ is the Euler's constant, $\gamma = 0.577215\dots$. To compute the Fourier coefficients of $G(x)$ efficiently and accurately, we note that the Fourier series of the logarithmic periodic function $\ln \left(\kappa a \left| \sin \frac{x}{2} \right| \right)$ in (17) is⁶ :

$$\ln \left(\kappa a \left| \sin \frac{x}{2} \right| \right) = \ln \left(\frac{\kappa a}{2} \right) - \sum_{n=1}^{\infty} \frac{\cos(nx)}{n} \quad (18)$$

Thus we can “subtract out” the singularity in $G(x)$ by forming

$$\overline{G}(x) = \frac{i}{4} H_0^{(1)} \left(2\kappa a \left| \sin \frac{x}{2} \right| \right) + \frac{1}{2\pi} \ln \left(\kappa a \left| \sin \frac{x}{2} \right| \right) J_0 \left(2\kappa a \left| \sin \frac{x}{2} \right| \right) \quad (19)$$

and then writing the Green's function as

$$G(x) = \overline{G}(x) - \frac{1}{2\pi} \ln \left(\kappa a \left| \sin \frac{x}{2} \right| \right) J_0 \left(2\kappa a \left| \sin \frac{x}{2} \right| \right) \quad (19')$$

It is easy to see that $\overline{G}(x)$ is finite for all values of x . Furthermore, both $\overline{G}(x)$ and $J_0 \left(2\kappa a \left| \sin \frac{x}{2} \right| \right)$ in (19') are periodic and infinitely differentiable. Thus their Fourier coefficients can be computed with spectral accuracy using FFT. The Fourier coefficients of the Green's function $G(x)$, g_n , will be computed according to (19') where the term involving the logarithmic function is computed by using convolution sums.

We now study the non-smoothness of the normal derivative of the Green's function $\frac{\partial G}{\partial \mathbf{n}}(x)$. The asymptotic series of the Bessel functions of first order for small argument are⁹ :

$$J_1(z) = \frac{z}{2} - \frac{z^3}{16} + \dots$$

$$Y_1(z) = -\frac{2}{\pi z} + \frac{2}{\pi} \ln \left(\frac{z}{2} \right) J_1(z) + \frac{2\gamma - 1}{2\pi} z - \dots$$

Then

$$\begin{aligned}
\frac{\partial G}{\partial \mathbf{n}}(x) &= -\frac{i\kappa}{4} H_1^{(1)}\left(2\kappa a \left|\sin \frac{x}{2}\right|\right) \left|\sin \frac{x}{2}\right| \\
&= -\frac{i\kappa}{4} \left[J_1\left(2\kappa a \left|\sin \frac{x}{2}\right|\right) + iY_1\left(2\kappa a \left|\sin \frac{x}{2}\right|\right) \right] \left|\sin \frac{x}{2}\right| \\
&= -\frac{1}{4\pi a} + \frac{\kappa}{2\pi} \ln\left(\kappa a \left|\sin \frac{x}{2}\right|\right) J_1\left(2\kappa a \left|\sin \frac{x}{2}\right|\right) \left|\sin \frac{x}{2}\right| + O(x^2) \quad (20)
\end{aligned}$$

Thus although $\frac{\partial G}{\partial \mathbf{n}}$ is a finite function, due to the logarithmic function appearing in the second term shown in (20), it does not have a smooth second derivative at $x = 0$. For this reason, its Fourier approximation will converge only at the rate of $1/N^3$.

The Fourier coefficients of $\frac{\partial G}{\partial \mathbf{n}}$, however, can be found easily using the relation to g_n given in Appendix A. In particular, we have

$$h_n = \begin{cases} -\frac{\kappa^2 a}{4n}(g_{n+1} - g_{n-1}) & n \neq 0, -\frac{N}{2}, \frac{N}{2} - 1 \\ \frac{\kappa^2 a}{4}(g_2 - g_0) - \frac{1}{a}g_1 & n = 0 \\ -\frac{\kappa^2 a}{4n}g_{-\frac{N}{2}+1} & n = -\frac{N}{2} \\ \frac{\kappa^2 a}{4n}g_{\frac{N}{2}-2} & n = \frac{N}{2} - 1 \end{cases} \quad (21)$$

Thus it is only necessary to compute g_n , the Fourier coefficients of $G(x)$.

C. Fast Fourier Transforms

The numerical implementation of computing g_n by (19') is given in this subsection.

Let us introduce Fourier collocation points

$$x_j = \frac{2\pi j}{N}, \quad j = 0, 1, 2, \dots, N-1$$

For convenience of discussion, denote the following Fourier series approximations

$$\bar{G}(x) = \sum_{n=-N/2}^{N/2-1} \bar{g}_n e^{-inx} \quad (22a)$$

$$J_0 \left(2\kappa a \left| \sin \frac{x}{2} \right| \right) = \sum_{n=-N/2}^{N/2-1} p_n e^{-inx} \quad (22b)$$

The coefficients of these expansions are computed by FFT (backward in the usual sense) as follows:

$$\bar{g}_n = \frac{1}{N} \sum_{j=0}^{N-1} \bar{G}(x_j) e^{inx_j} \quad (22a')$$

$$p_n = \frac{1}{N} \sum_{j=0}^{N-1} J_0 \left(2\kappa a \left| \sin \frac{x_j}{2} \right| \right) e^{inx_j} \quad (22b')$$

in which $\bar{G}(x_j)$ is computed by (19). For the value of $\bar{G}(x)$ at $x = 0$, the following limit, obtained from (17), can be used :

$$\bar{G}(0) = -\frac{\gamma}{2\pi} + \frac{i}{4}$$

In addition, we denote (18) as

$$\ln \left(\kappa a \left| \sin \frac{x}{2} \right| \right) = \sum_{n=-\infty}^{\infty} a_n e^{-inx} \quad (22c)$$

where $a_0 = \ln \left(\frac{\kappa a}{2} \right)$ and $a_n = -\frac{1}{2|n|}$ for $n \neq 0$.

Then, by (19'), the Fourier coefficients of $G(x)$ is computed as

$$g_n = \bar{g}_n - \frac{1}{2\pi} u_n \quad (23)$$

where u_n is the convolution sum :

$$u_n = \sum_{m=-N/2}^{N/2-1} p_m a_{n-m} \quad (24)$$

We note that the convolution sums in (24) require N multiplications for each u_n . Thus the total operations for the convolution sums are of order $O(N^2)$. This cost can

be reduced considerably to $O(N \log_2 N)$ by the use of a pseudospectral transformation method with de-aliasing techniques^{7,8}. For completeness, evaluation of (24) with a “padding” de-aliasing technique is given in Appendix B.

III. SPECTRAL METHOD FOR NEUMANN BOUNDARY CONDITIONS

We now discuss the Fourier spectral method for the Boundary Integral Equation (8b) of the Neumann boundary conditions. Upon substituting the truncated Fourier series of the layer distribution function $f(\theta)$ into (8b), we get

$$\frac{i\eta}{2} \sum_{n=-N/2}^{N/2-1} f_n e^{in\theta'} + \sum_{n=-N/2}^{N/2-1} \left[f_n \int_0^{2\pi} \left(\frac{\partial^2 G}{\partial \mathbf{n}' \partial \mathbf{n}} - i\eta \frac{\partial G}{\partial \mathbf{n}'} \right) e^{in\theta} a d\theta \right] = \sum_{n=-N/2}^{N/2-1} b_n e^{in\theta'} \quad (25)$$

where b_n are the Fourier coefficients of the specified Neumann boundary condition.

Again the integral appearing in equation (25) is directly related to the Fourier coefficients of $\frac{\partial^2 G}{\partial \mathbf{n}' \partial \mathbf{n}}$ and $\frac{\partial G}{\partial \mathbf{n}'}$. It is easy to find that the Fourier coefficients of $\frac{\partial G}{\partial \mathbf{n}'}$ are the same as those of $\frac{\partial G}{\partial \mathbf{n}}$, already given in the previous section as h_n . The apparent difficulty here is with the second normal derivative of the Green's function $\frac{\partial^2 G}{\partial \mathbf{n}' \partial \mathbf{n}}$. It can be shown that this function is strongly singular at $x = 0$ and, indeed, is not integrable in the ordinary sense. Fortunately it can also be shown that the integral with the second normal derivative can be transformed into one involving *tangential* derivatives with reduced singularity. In particular, we have¹⁰

$$\int_0^{2\pi} \frac{\partial^2 G}{\partial \mathbf{n}' \partial \mathbf{n}} e^{in\theta} a d\theta = \int_0^{2\pi} \left[\frac{1}{a} \frac{\partial e^{in\theta}}{\partial \theta} \frac{1}{a} \frac{\partial G}{\partial \theta'} + \kappa^2 \mathbf{n}' \cdot \mathbf{n} G e^{in\theta} \right] a d\theta \quad (26)$$

where $\frac{1}{a} \frac{\partial}{\partial \theta}$ and $\frac{1}{a} \frac{\partial}{\partial \theta'}$ represent tangential derivatives on the boundary.

The right hand side of (26) is now integrable in the sense of Cauchy Principal Value. To show this, we only need to note that by the expression of the Green's function given

in (6) we get

$$\begin{aligned}\frac{\partial G}{\partial \theta'} &= -\frac{i}{4} \frac{\partial}{\partial x} H_0^{(1)} \left(2\kappa a \left| \sin \frac{x}{2} \right| \right) = \frac{i\kappa a}{2} H_1^{(1)} \left(2\kappa a \left| \sin \frac{x}{2} \right| \right) \frac{\partial}{\partial x} \left| \sin \frac{x}{2} \right| \\ &= \frac{i\kappa a}{8} H_1^{(1)} \left(2\kappa a \left| \sin \frac{x}{2} \right| \right) \frac{\sin x}{\left| \sin \frac{x}{2} \right|}\end{aligned}\quad (27)$$

Recalling (20), the asymptotic expression of $\frac{\partial G}{\partial \theta'}$ for small x is found as

$$\frac{\partial G}{\partial \theta'} = \frac{\sin x}{8\pi \left| \sin \frac{x}{2} \right|^2} - \frac{\kappa a}{4\pi} \ln \left(\kappa a \left| \sin \frac{x}{2} \right| \right) J_1 \left(2\kappa a \left| \sin \frac{x}{2} \right| \right) \frac{\sin x}{\left| \sin \frac{x}{2} \right|} + O(x) \quad (28)$$

where $O(x)$ denotes smooth terms of order x and higher.

The singular first term shown above is integrable in the sense of the Cauchy Principal Value. In fact, we have

$$\frac{1}{2\pi} \int_0^{2\pi} \frac{\sin x}{\left| \sin \frac{x}{2} \right|^2} e^{inx} dx = \begin{cases} 0 & \text{when } n = 0 \\ 2i \operatorname{sign}(n) & \text{when } n \neq 0 \end{cases} \quad (29)$$

Upon substituting $x = \theta - \theta'$ and equating the coefficients of $e^{in\theta'}$, equation (25) is reduced to

$$\frac{i\eta}{2} f_n + f_n \int_0^{2\pi} \left(\frac{in}{a^2} \frac{\partial G}{\partial \theta'}(x) + \kappa^2 \cos(x) G(x) - i\eta \frac{\partial G}{\partial \mathbf{n}'}(x) \right) e^{inx} a dx = b_n \quad (30)$$

in which we have used the fact that, for a circular cylinder,

$$\mathbf{n}' \cdot \mathbf{n} = \cos(\theta - \theta')$$

The integral in (30) will now be evaluated through the Fourier coefficients of each term.

For the first term, the Fourier coefficients of $\frac{\partial G}{\partial \theta'}$ are obtained from the relation

$$\frac{\partial G}{\partial \theta'} = -\frac{\partial G}{\partial x} = \sum_{n=-N/2}^{N/2-1} in g_n e^{-inx} \quad (31)$$

where g_n are the Fourier coefficients of $G(x)$ by (13).

The Fourier series approximation of the second term in the integral of (30) can also be found using g_n since we have

$$\cos(x) G(x) = \cos(x) \sum_{n=-N/2}^{N/2-1} g_n e^{-inx} \approx \sum_{n=-N/2}^{N/2-1} \tilde{g}_n e^{-inx} \quad (32)$$

where

$$\tilde{g}_n = \begin{cases} \frac{1}{2}g_{-\frac{N}{2}+1} & n = -N/2 \\ \frac{1}{2}(g_{n-1} + g_{n+1}) & -N/2 + 1 \leq n \leq N/2 - 2 \\ \frac{1}{2}g_{\frac{N}{2}-2} & n = N/2 - 1 \end{cases} \quad (33)$$

Hence equation (30) is reduced to the following algebraic equations

$$\frac{i\eta}{2}f_n + 2\pi a f_n \left(-\frac{n^2}{a^2}g_n + \kappa^2 \tilde{g}_n - i\eta h_n \right) = b_n \quad (34)$$

for $-N/2 \leq n \leq N/2 - 1$.

Therefore, the Fourier coefficients of the layer distribution function $f(\theta)$ for the Neumann boundary conditions are obtained *explicitly* as

$$f_n = \frac{b_n}{\frac{i\eta}{2} + 2\pi a \left(-\frac{n^2}{a^2}g_n + \kappa^2 \tilde{g}_n - i\eta h_n \right)} \quad (35)$$

where g_n , \tilde{g}_n and h_n are computed by (23), (33), and (21), respectively.

We point out, however, that \tilde{g}_n as given by (33) and, indeed, h_n of (21), are not exact for $n = -N/2$ and $N/2 - 1$, owing to a truncated series of $G(x)$ in the computation. Whereas it is possible to compute these two coefficients exactly, the resulting error in the last two coefficients of f_n is negligible because b_n , in the numerator, decays exponentially as for smooth boundary conditions. That is, f_n for $n = -N/2$ and $N/2 - 1$ are necessarily negligibly small if N is sufficiently large. For simplicity and practicality, (21) and (33) are retained in the numerical calculations.

IV. NUMERICAL EXAMPLES

In this section, numerical results of a plane wave scattering by a circular cylinder are presented. The incident wave is assumed to be

$$\phi_i = e^{i\kappa x}$$

The scattered wave, ϕ , satisfies the Helmholtz equation (1). The boundary conditions considered here are the Dirichlet type $\phi = -\phi_i$ and the Neumann type $\frac{\partial\phi}{\partial\mathbf{n}} = -\frac{\partial\phi_i}{\partial\mathbf{n}}$.

The solutions for the scattered field are obtained by the layer representation (2) as

$$\begin{aligned}\phi(\vec{r}') &= \int_0^{2\pi} \left(\frac{\partial G}{\partial \mathbf{n}} - i\eta G \right) f(\theta) a d\theta \\ &= a \sum_{n=-N/2}^{N/2-1} f_n \int_0^{2\pi} \left(\frac{\partial G}{\partial \mathbf{n}} - i\eta G \right) e^{in\theta} d\theta\end{aligned}$$

The above integral can be easily evaluated directly using FFT, since the Green's function has no singularity for points lying outside of the boundary. The details are omitted here.

For plane incident waves, exact solution is given by infinite series of the Bessel and Hankel functions⁶. Our purpose here is to demonstrate the exponential rate of convergence of the numerical solutions. We emphasize again that the numerical formulation applies to any form of the incident waves. Due to its simplicity, a sample FORTRAN program is listed in Appendix C.

In numerical calculations, the radius of the cylinder, a , is taken to be 1 and also $\eta = 1$. Computations for $\kappa a = 1, 10$ and 100 have been carried out. In Tables I to IV, numerical values of the layer distribution function $f(\theta)$ and the scattered function ϕ at far field are given for selected points in space. Exact values at far field are also shown in the tables. Clearly as the number of Fourier collocation points increases, the

numerical solution converges exponentially fast. Significant improvements in accuracy are observed with relatively small increase of the number of datum points. This is often true for spectral methods in general. The error decreases dramatically when the number of points is large enough to resolve the basic features of the solution.

The corresponding layer distribution function $f(\theta)$ is plotted in Figures 1 to 6 for the Dirichlet and Neumann boundary conditions for $\kappa a = 1, 10$ and 100 . These graphs demonstrate again the remarkable accuracy of the Fourier spectral methods with relatively small number of datum points.

Far field scattered intensities, computed as $|\vec{r}|\phi^2$, are plotted in Figure 8 and 9 for the Dirichlet and Neumann boundary conditions, respectively.

V. CONCLUSIONS

A fast numerical solution of wave scattering by a circular cylinder has been presented. It is shown that by properly removing the non-smoothness of the integral kernels of the Boundary Integral Equations, Spectrally accurate numerical solutions are obtained. The numerical error decays exponentially as the number of datum points increase. This implies that the present method requires significantly fewer points for achieving a given accuracy in comparison with previous numerical approaches. The present method is also easy to implement.

Moreover, the combined single and double-layer formulation of the Boundary Integral Equations ensures the uniqueness of the numerical solution for all frequencies. It is shown that the hypersingularity of the Boundary Integral Equations can be handled easily in the spectral method.

APPENDIX

A. Exact expressions of g_n and h_n

In this appendix we derive the exact analytic expressions for the Fourier coefficients of $G(x)$ and $\frac{\partial G}{\partial \mathbf{n}}(x)$.

It can be shown that, e.g. by (7.2.51) of ref. 6,

$$H_0^{(1)}\left(2\kappa a \left|\sin \frac{x}{2}\right|\right) = \sum_{m=-\infty}^{\infty} H_m^{(1)}(\kappa a) J_m(\kappa a) e^{-imx} \quad (A1)$$

Hence

$$\begin{aligned} g_n &= \frac{1}{2\pi} \int_0^{2\pi} G(x) e^{inx} dx \\ &= \frac{1}{2\pi} \int_0^{2\pi} \frac{i}{4} H_0^{(1)}\left(2\kappa a \left|\sin \frac{x}{2}\right|\right) e^{inx} dx \\ &= \frac{i}{4} H_n^{(1)}(\kappa a) J_n(\kappa a) \end{aligned}$$

Moreover, for $n \neq 0$, using integration by part and (A1),

$$\begin{aligned} h_n &= \frac{1}{2\pi} \int_0^{2\pi} \frac{\partial G}{\partial \mathbf{n}}(x) e^{inx} dx \\ &= -\frac{i\kappa}{8\pi} \int_0^{2\pi} H_1^{(1)}\left(2\kappa a \left|\sin \frac{x}{2}\right|\right) \left|\sin \frac{x}{2}\right| e^{inx} dx \\ &= \frac{\kappa^2 a}{4\pi n} \int_0^{2\pi} H_0^{(1)}\left(2\kappa a \left|\sin \frac{x}{2}\right|\right) \left|\sin \frac{x}{2}\right| \cos \frac{x}{2} e^{inx} dx \\ &= \frac{\kappa^2 a}{8\pi n} \int_0^{2\pi} \left[\sum_{m=-\infty}^{\infty} H_m^{(1)}(\kappa a) J_m(\kappa a) e^{-imx} \right] \sin x e^{inx} dx \\ &= -\frac{\kappa^2 a i}{16n} \left[H_{n+1}^{(1)}(\kappa a) J_{n+1}(\kappa a) - H_{n-1}^{(1)}(\kappa a) J_{n-1}(\kappa a) \right] \\ &= -\frac{\kappa^2 a}{4n} (g_{n+1} - g_{n-1}) \end{aligned}$$

where use has been made of the formula⁹

$$\frac{d}{dz} \left[z H_1^{(1)}(z) \right] = z H_0^{(1)}(z)$$

For $n = 0$, further calculations show that

$$\begin{aligned} h_0 &= \frac{\kappa^2 a i}{16} \left[H_2^{(1)}(\kappa a) J_2(\kappa a) - H_0^{(1)}(\kappa a) J_0(\kappa a) \right] - \frac{i}{4a} H_1^{(1)}(\kappa a) J_1(\kappa a) \\ &= \frac{\kappa^2 a}{4} (g_2 - g_0) - \frac{1}{a} g_1 \end{aligned}$$

B. Evaluation of convolution sums

An algorithm of computing convolution sums u_n with $O(N \log_2 N)$ operations is shown below⁸.

Let $M \geq 3N$ and

$$\xi_j = 2\pi j/M, \quad j = 0, 1, 2, \dots, M-1$$

Compute the following using FFT for $j = 0, 1, 2, \dots, M-1$:

$$A_j = \sum_{m=-M/2}^{M/2-1} \tilde{a}_m e^{-im\xi_j}$$

$$P_j = \sum_{m=-M/2}^{M/2-1} \tilde{p}_m e^{-im\xi_j}$$

where

$$\tilde{a}_m = \begin{cases} a_m & -N \leq m \leq N-1 \\ 0 & \text{other} \end{cases}$$

$$\tilde{p}_m = \begin{cases} p_m & -N/2 \leq m \leq N/2-1 \\ 0 & \text{other} \end{cases}$$

and form the product

$$U_j = A_j P_j$$

Then the convolution sum u_n is the (backward) FFT of U_j as follows

$$u_n = \frac{1}{M} \sum_{j=0}^{M-1} U_j e^{in\xi_j}$$

for $-N/2 \leq n \leq N/2 - 1$.

C. FORTRAN program

A FORTRAN program of implementing the Fourier spectral method is listed below. (The routines *cftti*, *cfttf* and *cfttb* denote initialization, forward and backward FFT transforms respectively.)

```
      program circle
c*****
c n : number of points; isoft=1 : Dirichlet B.C.; isoft=0 : Neumann B.C.
c*****
      parameter(n=32,ak=10.0,isoft=1,eta=1.0,n1=n-1,nhalf=n/2,m=3*n,
> rn=float(n),pi=3.14159265358979324,euler=0.57721566490153286)
      complex b(0:n1),fn(0:n1),gbar(0:n1),gn(0:n1),hn(0:n1),p(0:n1),
> gtilde(0:n1),am(0:m-1),pm(0:m-1),wsave(2000),wsave2(2000),ei,phi
      ei=(0.0,1.0)
      call cftti(n,wsave)
      call getbc(n,ak,b,ei,pi)
      call cfttf(n,b,wsave)
      do 10 j=0,n-1
         tmp=2.0*ak*abs(sin(pi*float(j)/rn))
         if(j.eq.0) then
            gbar(0)=-euler/2.0/pi+ei/4.0
            p(0)=1.0
         else
            gbar(j)=ei/4.0*(besj0(tmp)+ei*besy0(tmp))
>            +0.5*aalog(tmp/2.0)*besj0(tmp)/pi
            p(j)=besj0(tmp)
         endif
10      continue
      call cfttb(n,gbar,wsave)
      call cfttb(n,p,wsave)
      am(0)=aalog(ak/2.0)
      am(2*n)=-1.0/2.0/rn
      do 21 i=1,n-1
         am(i)=-1.0/2.0/float(i)
21      am(2*n+i)=1.0/2.0/float(i-n)
      do 22 i=0,nhalf-1
         pm(i)=p(i)
22      pm(5*nhalf+i)=p(nhalf+i)
      call cftti(m,wsave2)
      call cfttf(m,am,wsave2)
      call cfttf(m,pm,wsave2)
      do 23 j=0,m-1
23      pm(j)=am(j)*pm(j)
      call cfttb(m,pm,wsave2)
      do 31 i=0,nhalf-1
```

```

      gn(i)=gbar(i)-0.5*pm(i)/float(m)/pi
31      gn(nhalf+i)=gbar(nhalf+i)-0.5*pm(5*nhalf+i)/float(m)/pi
      hn(0)=ak**2/4.0*(gn(2)-gn(0))-gn(1)
      hn(nhalf-1)=ak**2/4.0/float(nhalf-1)*gn(nhalf-2)
      hn(nhalf)=ak**2/4.0/float(nhalf)*gn(nhalf+1)
      hn(n-1)=ak**2/4.0*(gn(0)-gn(n-2))
      gtilde(0)=0.5*(gn(1)+gn(n-1))
      gtilde(nhalf-1)=0.5*gn(nhalf-2)
      gtilde(nhalf)=0.5*gn(nhalf+1)
      gtilde(n-1)=0.5*(gn(0)+gn(n-2))
      do 32 i=1,n-2
          itrue=i
          if(i.ge.nhalf) itrue=i-n
          if(i.eq.nhalf-1.or.i.eq.nhalf) go to 32
          hn(i)=-ak**2/4.0/float(itrue)*(gn(i+1)-gn(i-1))
          gtilde(i)=0.5*(gn(i-1)+gn(i+1))
32      continue
      do 40 i=0,n-1
          if(isoft.eq.1) then
              fn(i)=b(i)/(0.5*rn+2.0*pi*(hn(i)-ei*eta*gn(i)))
          else
              itrue=i
              if(i.ge.nhalf) itrue=i-n
              fn(i)=b(i)/(0.5*ei*eta*rn+2.0*pi*(-float(itrue)**2*gn(i)
>                  +ak**2*gtilde(i)-ei*eta*hn(i)))
          endif
40      continue
c*****
c The following is to find phi at far field r=r0
c*****
      r0=10.0
      npoint=4
      do 70 ii=1,npoint
          sj=2.0*pi*float(ii-1)/float(npoint)
          do 71 j=0,n-1
              theta=2.0*pi*float(j)/rn
              rj=sqrt(1.0+r0*r0-2.0*r0*cos(theta-sj))
              dj=1.0-r0*cos(theta-sj)
              tmp=ak*rj
              gn(j)=ei/4.0*(besj0(tmp)+ei*besy0(tmp))
71          hn(j)=-ei*ak/4.0*(besj1(tmp)+ei*besy1(tmp))*dj/rj
          call cfftb(n,gn,wsave)
          call cfftb(n,hn,wsave)
          phi=0.0
          do 72 i=0,n-1
72          phi=phi+2.0*pi*fn(i)*(hn(i)-ei*eta*gn(i))/rn
70          write(3,100) r0,sj,phi,cabs(phi)
100          format(' r0=',e15.6,' theta=',e15.6/'      phi=',3e17.10)
999      stop
      end
c
      subroutine getbc(n,ak,b,ei,pi)
      complex ei,b(0:n-1),tmp
      do 10 j=0,n-1

```



```

10      tmp=ei*ak*cos(2.0*pi*float(j)/float(n))
        b(j)=-cexp(tmp)
        return
        end

```

ACKNOWLEDGEMENTS

The author wishes to thank Dr. D.G. Lasseigne for helpful comments and discussions.

REFERENCES

- ¹D. Colton and R. Kress, *Integral Equation Methods In Scattering Theory*, Wiley-Interscience, 1983.
- ²C. A. Brebbia and M. S. Ingber, *Boundary Element Technology VII*, Elsevier, 1992.
- ³N. N. Bojarski, "Scattering by a cylinder: A fast exact numerical solution," *J. Acoust. Soc. Amer.* **75**(2), 320-323, 1984.
- ⁴G. T. Schuster, "A fast exact numerical solution for the acoustic response of concentric cylinders with penetrable interfaces." *J. Acoust. Soc. Amer.* **87**(2), 495-502, 1990.
- ⁵G. Chen and J. Zhou, *Boundary Element Methods*, Academic Press, 1992.
- ⁶P. Morse and H. Feshbach, *Methods of Theoretical Physics*, McGraw-Hill, 1953.
- ⁷D. Gottlieb and S. Orszag, *Numerical Analysis of Spectral Methods : Theory and Applications*, SIAM, 1977.
- ⁸C. Canuto, M. Y. Hussaini, A. Quarteroni and T. A. Zang, *Spectral Methods in Fluid Dynamics*, Springer-Verlag, 1988.
- ⁹M. Abramowitz and I. A. Stegun, *Handbook of Mathematical Functions*, Dover, 1965.
- ¹⁰A. J. Burton and G. F. Miller, "The application of integral equation methods to the numerical solution of some exterior boundary-value problems", *Proc. Roy. Soc. Lond. A*, **323**, 201-210, 1971.

TABLE I

Values of the layer distribution function $f(\theta)$ at selected points on the boundary. Dirichlet boundary condition.

N	$\theta = 0^\circ$	$\theta = 90^\circ$	$\theta = 180^\circ$	Error
$\kappa a = 1$				
4	1.101447573	1.102982967	1.124378820	10^{-2}
8	1.113205176	1.095419894	1.146430615	10^{-3}
16	1.112753432	1.094877536	1.145739275	10^{-8}
24	1.112753420	1.094877525	1.145739263	10^{-12}
$\kappa a = 10$				
24	4.590213453	6.904710445	5.180354736	10^{-2}
32	4.546357630	6.901732036	5.132718905	10^{-3}
48	4.545461066	6.901500667	5.132515158	10^{-8}
56	4.545461055	6.901500659	5.132515156	10^{-12}
$\kappa a = 100$				
224	20.64255659	6.841653547	18.93255934	10^{-3}
256	20.64325731	6.842244857	18.93221646	10^{-9}
512	20.64325733	6.842244863	18.93221644	10^{-12}

TABLE II

Values of the scattered function ϕ at selected points
at far field $r = 10a$. Dirichlet boundary condition.

N	$\theta = 0^\circ$	$\theta = 90^\circ$	$\theta = 180^\circ$	Error
$\kappa a = 1$				
4	0.4146449903	0.2787718545	0.1852248716	10^{-2}
8	0.4224209076	0.2612785029	0.2551151985	10^{-4}
16	0.4224153154	0.2613031445	0.2552183381	10^{-10}
Exact	0.4224153154	0.2613031445	0.2552183381	—
$\kappa a = 10$				
24	0.8255952003	0.1969679200	0.1864749710	10^{-2}
32	0.8285176644	0.1953580665	0.2300067055	10^{-4}
48	0.8285110664	0.1953543814	0.2300939707	10^{-10}
Exact	0.8285110664	0.1953543814	0.2300939707	—
$\kappa a = 100$				
224	0.8562228283	0.1881301853	0.2295232548	10^{-3}
256	0.8562289911	0.1881326409	0.2294229274	10^{-10}
Exact	0.8562289911	0.1881326409	0.2294229274	—

TABLE III

Values of the layer distribution function $f(\theta)$ at selected points on the boundary. Neumann boundary condition.

N	$\theta = 0^\circ$	$\theta = 90^\circ$	$\theta = 180^\circ$	Error
$\kappa a = 1$				
4	1.035182633	0.3028073027	0.8616587030	10^{-1}
8	1.200134116	0.3972281648	0.8518411247	10^{-2}
16	1.199187560	0.3963806796	0.8495643896	10^{-7}
24	1.199187560	0.3963806589	0.8495643587	10^{-12}
$\kappa a = 10$				
24	0.6004486353	0.4814454225	1.362228889	10^{-1}
32	0.6274625969	0.6575899642	1.577833267	10^{-2}
48	0.6302381163	0.6567081358	1.460119442	10^{-7}
56	0.6302381517	0.6567081198	1.460119455	10^{-12}
$\kappa a = 100$				
224	0.2185547081	1.282490390	2.054272775	10^{-2}
256	0.2157948725	1.283008634	2.057912965	10^{-7}
512	0.2157947803	1.283008643	2.057913072	10^{-12}

• **TABLE IV**

Values of the scattered function ϕ at selected points
at far field $r = 10a$. Neumann boundary condition.

N	$\theta = 0^\circ$	$\theta = 90^\circ$	$\theta = 180^\circ$	Error
$\kappa a = 1$				
4	0.1583300606	0.1690204144	0.1619964200	10^{-1}
8	0.1732916160	0.1563414831	0.2312523394	10^{-4}
16	0.1733358919	0.1563260243	0.2313583724	10^{-10}
Exact	0.1733358919	0.1563260243	0.2313583724	—
$\kappa a = 10$				
24	0.7679584467	0.2167643382	0.1574136977	10^{-1}
32	0.7740714632	0.1956069424	0.2282238894	10^{-3}
48	0.7740874173	0.1955960691	0.2283394143	10^{-10}
Exact	0.7740874173	0.1955960691	0.2283394143	—
$\kappa a = 100$				
224	0.7688015277	0.1871656432	0.2295250315	10^{-3}
256	0.7688018590	0.1871717295	0.2293995512	10^{-10}
Exact	0.7688018590	0.1871717295	0.2293995512	—

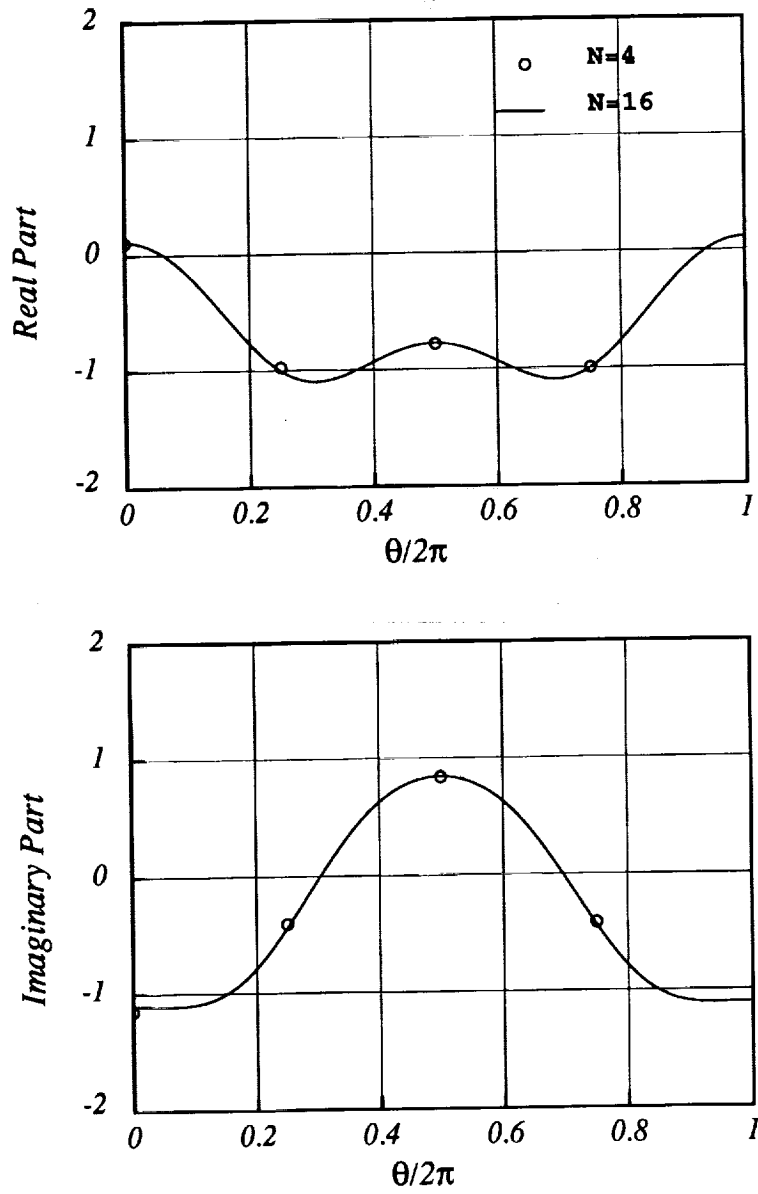


Figure 1. Layer distribution function $f(\theta)$ for $\kappa a = 1$. Dirichlet boundary condition.

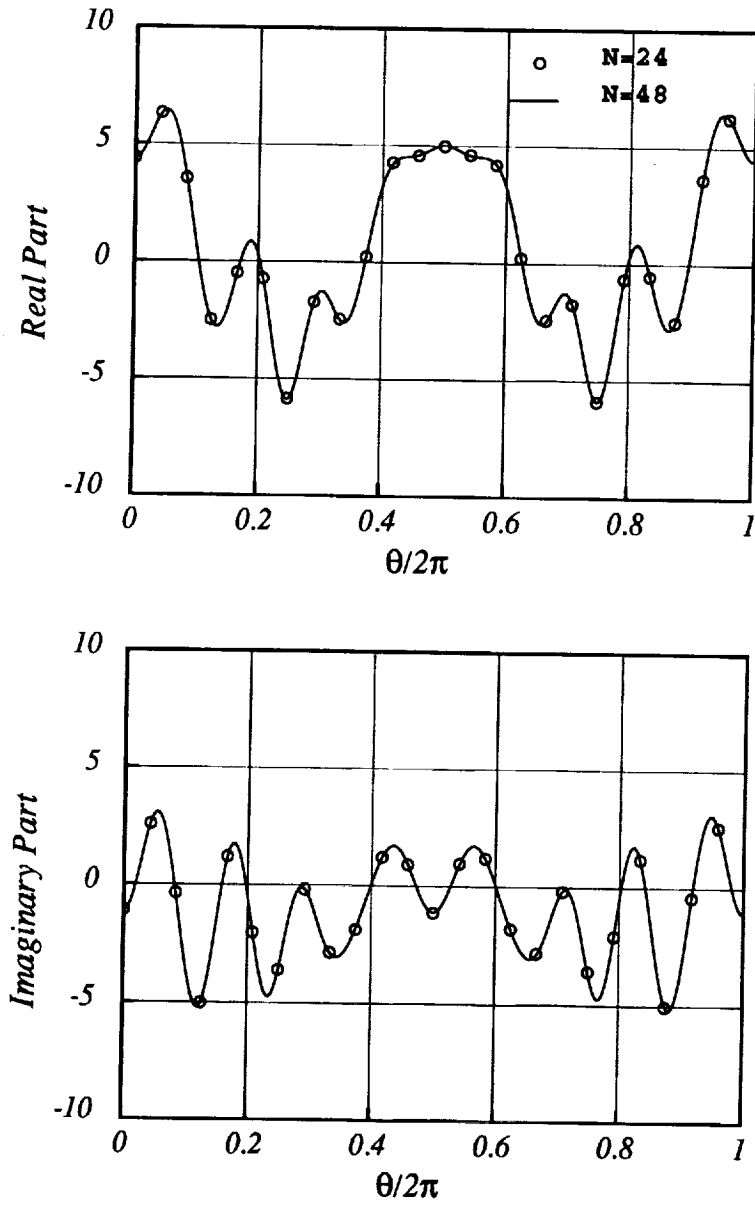


Figure 2. Layer distribution function $f(\theta)$ for $\kappa a = 10$. Dirichlet boundary condition.

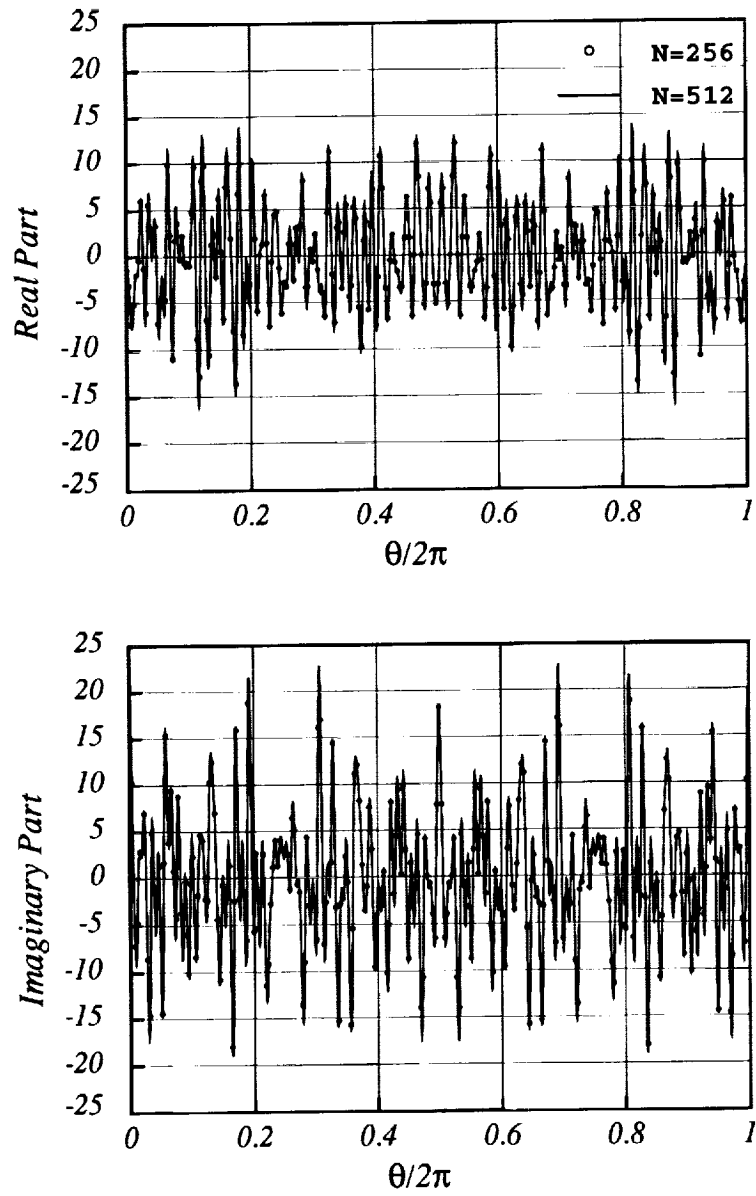


Figure 3. Layer distribution function $f(\theta)$ for $\kappa a = 100$. Dirichlet boundary condition.

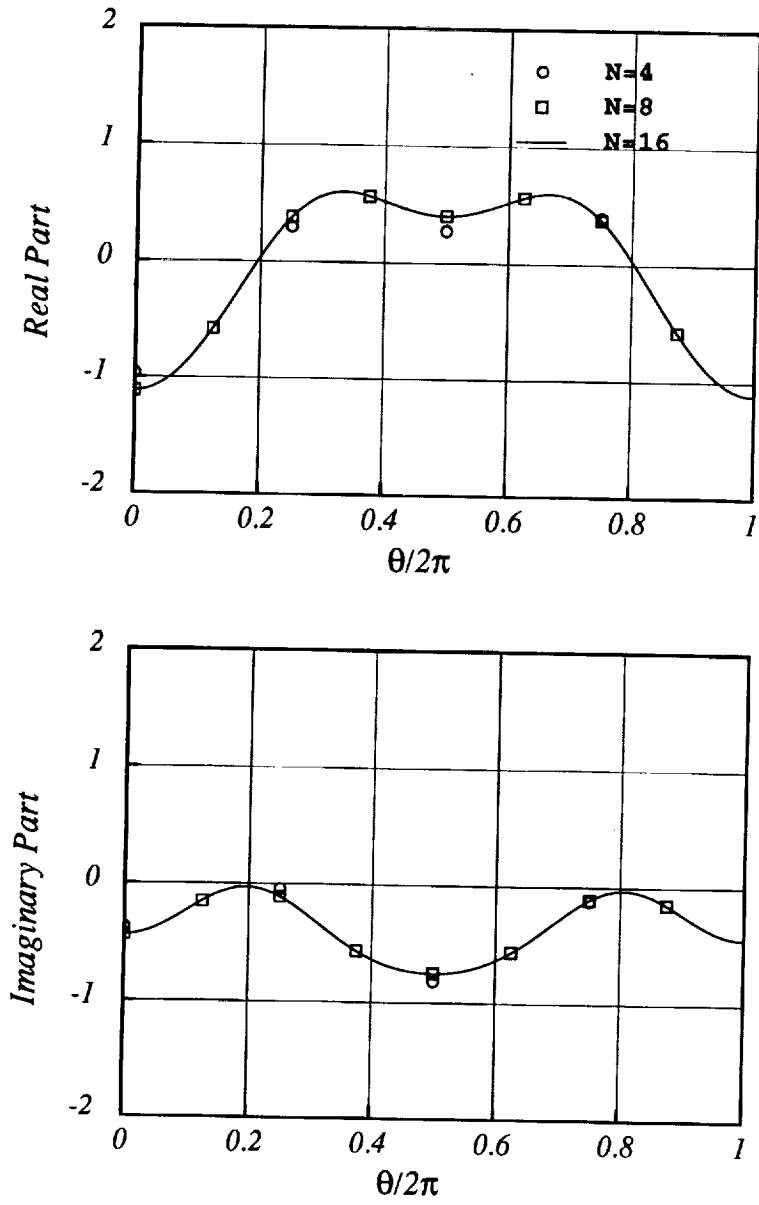


Figure 4. Layer distribution function $f(\theta)$ for $\kappa a = 1$. Neumann boundary condition.

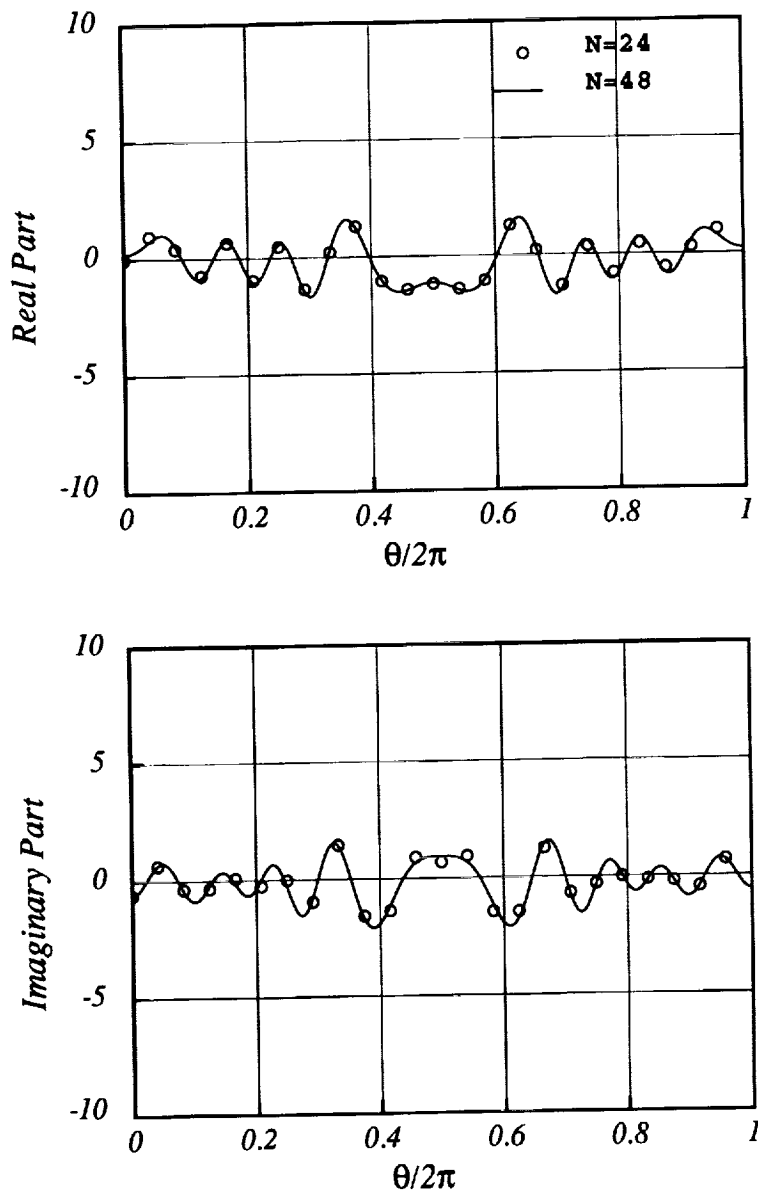


Figure 5. Layer distribution function $f(\theta)$ for $\kappa a = 10$. Neumann boundary condition.

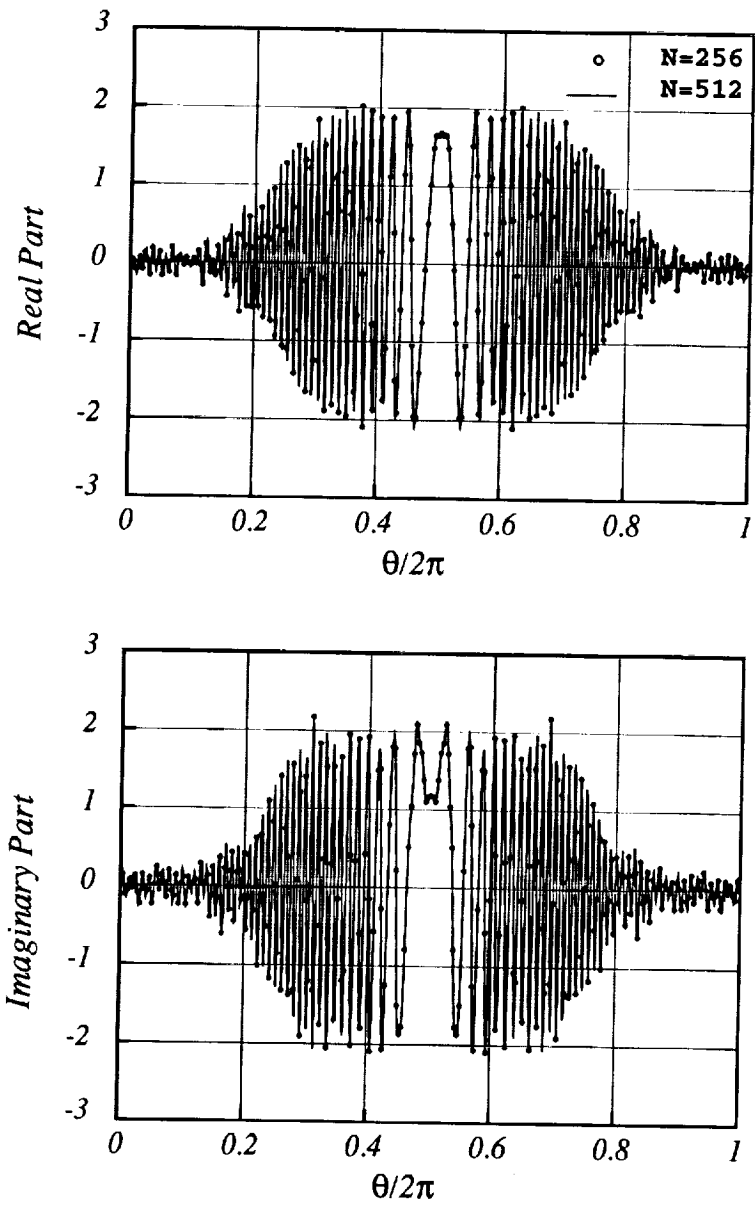


Figure 6. Layer distribution function $f(\theta)$ for $\kappa a = 100$. Neumann boundary condition.

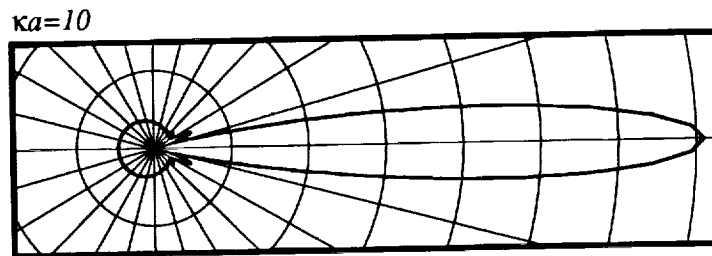
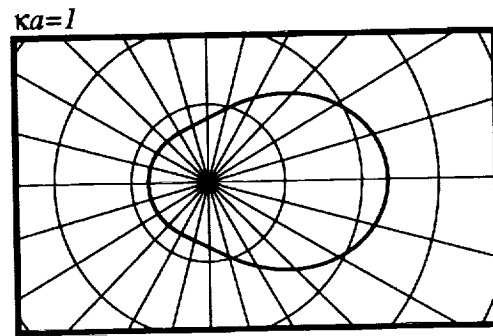


Figure 7. Directivities of the far field scattered function, Dirichlet boundary condition.

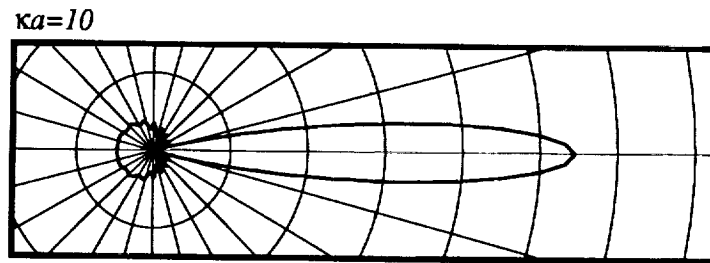
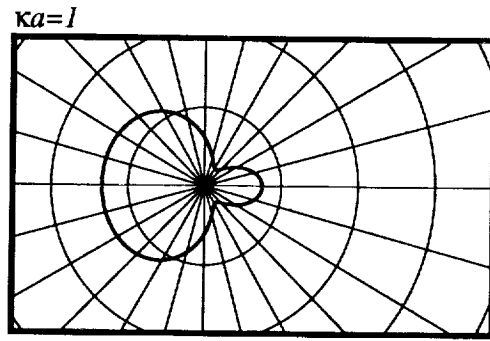


Figure 8. Directivities of the far field scattered function, Neumann boundary condition.

REPORT DOCUMENTATION PAGE			Form Approved OMB No. 0704-0188	
Public reporting burden for this collection of information is estimated to average 1 hour per response, including the time for reviewing instructions, searching existing data sources, gathering and maintaining the data needed, and completing and reviewing the collection of information. Send comments regarding this burden estimate or any other aspect of this collection of information, including suggestions for reducing this burden, to Washington Headquarters Services, Directorate for Information Operations and Reports, 1215 Jefferson Davis Highway, Suite 1204, Arlington, VA 22202-4302, and to the Office of Management and Budget, Paperwork Reduction Project (0704-0188), Washington, DC 20503.				
1. AGENCY USE ONLY(Leave blank)	2. REPORT DATE May 1994	3. REPORT TYPE AND DATES COVERED Contractor Report		
4. TITLE AND SUBTITLE A FAST NUMERICAL SOLUTION OF SCATTERING BY A CYLINDER: SPECTRAL METHOD FOR THE BOUNDARY INTEGRAL EQUATIONS			5. FUNDING NUMBERS C NAS1-19480 WU 505-90-52-01	
6. AUTHOR(S) Fang Q. Hu				
7. PERFORMING ORGANIZATION NAME(S) AND ADDRESS(ES) Institute for Computer Applications in Science and Engineering Mail Stop 132C, NASA Langley Research Center Hampton, VA 23681-0001			8. PERFORMING ORGANIZATION REPORT NUMBER ICASE Report No. 94-36	
9. SPONSORING/MONITORING AGENCY NAME(S) AND ADDRESS(ES) National Aeronautics and Space Administration Langley Research Center Hampton, VA 23681-0001			10. SPONSORING/MONITORING AGENCY REPORT NUMBER NASA CR-194918 ICASE Report No. 94-36	
11. SUPPLEMENTARY NOTES Langley Technical Monitor: Michael F. Card Final Report Submitted to Journal of Acoustic Society of America				
12a. DISTRIBUTION/AVAILABILITY STATEMENT Unclassified-Unlimited Subject Category 34			12b. DISTRIBUTION CODE	
13. ABSTRACT (Maximum 200 words) It is known that the exact analytic solutions of wave scattering by a circular cylinder, when they exist, are not in a closed form but in a closed form but in infinite series which converges slowly for high frequency waves. In this paper, we present a fast numerical solution for the scattering problem in which the Boundary Integral Equations, reformulated from the Helmholtz equation, are solved using a Fourier spectral method. It is shown that the special geometry considered here allows the implementation of the spectral method to be simple and very efficient. The present method differs from previous approaches in that the singularities of the integral kernels are removed and dealt with accurately. The proposed method preserves the spectral accuracy and is shown to have an exponential rate of convergence. Aspects of efficient implementation using FFT are discussed. Moreover, the boundary integral equations of combined single and double-layer representation are used in the present paper. This ensures the uniqueness of the numerical solution for the scattering problem at all frequencies. Although a strongly singular kernel is encountered for the Neumann boundary conditions, we show that the hypersingularity can be handled easily in the spectral method. Numerical examples that demonstrate the validity of the method are also presented.				
14. SUBJECT TERMS Acoustic scattering, spectral method			15. NUMBER OF PAGES 37	
			16. PRICE CODE A03	
17. SECURITY CLASSIFICATION OF REPORT Unclassified	18. SECURITY CLASSIFICATION OF THIS PAGE Unclassified	19. SECURITY CLASSIFICATION OF ABSTRACT	20. LIMITATION OF ABSTRACT	